Journal of Inorganic Biochemistry 118 (2013) 100–106

Contents lists available at SciVerse ScienceDirect

Journal of Inorganic Biochemistry

journal homepage: www.elsevier.com/locate/jinorgbio

Structure and spectroscopy of a bidentate *bis*-homocitrate dioxo-molybdenum(VI) complex: Insights relevant to the structure and properties of the FeMo-cofactor in nitrogenase

Zhao-Hui Zhou [a,b,c,*], Hongxin Wang [a,b], Ping Yu [d], Marilyn M. Olmstead [a], Stephen P. Cramer [a,b,*]

[a] Department of Chemistry, University of California, Davis, CA 95616, United States
[b] Physical Biosciences Division, Lawrence Berkeley National Laboratory, Berkeley, CA 94720, United States
[c] State Key Laboratory for Physical Chemistry of the Solid Surfaces, Xiamen University, Xiamen 361005, China
[d] NMR Facility, University of California, Davis, CA 95616, United States

ARTICLE INFO

Article history:
Received 19 September 2012
Received in revised form 30 September 2012
Accepted 1 October 2012
Available online 8 October 2012

Keywords:
Homocitrate
FeMo-cofactor
Nitrogenase
Crystal structure

ABSTRACT

Direct reaction of potassium molybdate (with natural abundance Mo or enriched with ^{92}Mo or ^{100}Mo) with excess hydrolyzed homocitric acid-γ-lactone in acidic solution resulted in the isolation of a *cis*-dioxo *bis*-homocitrato molybdenum(VI) complex, $K_2[^*MoO_2(R,S\text{-}H_2homocit)_2]\cdot 2H_2O$ (**1**) (*Mo = Mo, **1**; ^{92}Mo, **2**; ^{100}Mo, **3**; H_4homocit = homocitric acid-γ-lactone·H_2O) and $K_2[MoO_2(^{18}O\text{-}R,S\text{-}H_2homocit)_2]\cdot 2H_2O$ (**4**). The complex has been characterized by elemental analysis, FT-IR, solid and solution ^{13}C NMR, and single crystal x-ray diffraction analysis. The molybdenum atom in (**1**) is *quasi*-octahedrally coordinated by two *cis* oxo groups and two bidentate homocitrate ligands. The latter coordinates *via* its α-alkoxy and α-carboxy groups, while the β- and γ-carboxylic acid groups remain uncomplexed, similar to the coordination mode of homocitrate in the Mo-cofactor of nitrogenase. In the IR spectra, the Mo=O stretching modes near 900 cm^{-1} show 2–3 cm^{-1} red- and blue-shifts for the ^{92}Mo-complex (**2**) and ^{100}Mo-complex (**3**) respectively compared with the natural abundance version (**1**). At lower frequencies, bands at 553 and 540 cm^{-1} are assigned to ν_{Mo-O} vibrations involving the alkoxide ligand. At higher frequencies, bands in the 1700–1730 cm^{-1} region are assigned to stretching modes of protonated carboxylates. In addition, a band at 1675 cm^{-1} was observed that may be analogous to a band seen at 1677 cm^{-1} in nitrogenase photolysis studies. The solution behavior of (**1**) in D_2O was probed with ^{1}H and ^{13}C NMR spectra. An obvious dissociation of homocitrate was found, even though bound to the high valent Mo(VI). This suggests the likely lability of coordinated homocitrate in the FeMo-cofactor with its lower valence Mo(IV).

1. Introduction

Homocitrate produced by the *nif*V gene product (homocitrate synthase) is a key ingredient in the complex *in vivo* biosynthesis of the FeMo-cofactor of nitrogenase [1–6]. X-ray crystallography has shown that homocitrate coordinates the active site Mo in a bidentate fashion through alkoxide and carboxylate ligands from the C-2 position, thus creating a 5-membered ring as shown in Fig. 1 [7–9]. Crystallographic analysis of nitrogenase from a *nifV* mutant shows that citrate can adopt a similar mode of binding [10], but the simple deletion of a single methylene group from the γ-carboxylate tail reduces N_2 reduction activity to only 7% that of wild-type enzyme [11]. Removal of homocitrate also results in an enzyme whose H_2-evolution activity, unlike the wild-type, is inhibited by CO [12]. Shah et al. investigated the ability of a wide range of homocitrate analogues to reconstitute enzyme activity, and concluded that the minimal requirements were the 'hydroxy group, the 1- and 2-carboxy groups, and the *R*-configuration of the chiral center' [13]. Thus, despite a great deal of evidence favoring Fe as the N_2 substrate binding metal [14] and the 4Fe-4S face neighboring the α-V70 sidechain of the *Av* MoFe protein as the binding location [15–18], there is something special about homocitrate ligation at the Mo end of the FeMo-cofactor that remains critical to the catalytic mechanism. For this reason we have investigated the structural and spectroscopic properties of a homocitrate ligated Mo complex.

In this work, we report the synthesis, x-ray diffraction structural characterization, FT-IR, and solid and solution NMR spectroscopy of a molybdenum(VI)-homocitrate complex isolated from aqueous solution. Isotopic substitution with ^{92}Mo and ^{100}Mo was used to confirm assignment of the vibrations involving molybdenum and oxygen, and ^{18}O substitution helped in assignment of certain free carboxylate modes. We also observed an equilibrium between coordinated and free homocitrate ligand in solution based on ^{13}C NMR technique, and the potential relevance to properties of homocitrate in nitrogenase is also discussed.

* Corresponding authors at: Department of Chemistry, University of California, Davis, CA 95616, United States.
E-mail addresses: zhzhou@xmu.edu.cn (Z.-H. Zhou), spjcramer@ucdavis.edu (S.P. Cramer).

0162-0134/$ – see front matter © 2012 Elsevier Inc. All rights reserved.
http://dx.doi.org/10.1016/j.jinorgbio.2012.10.001

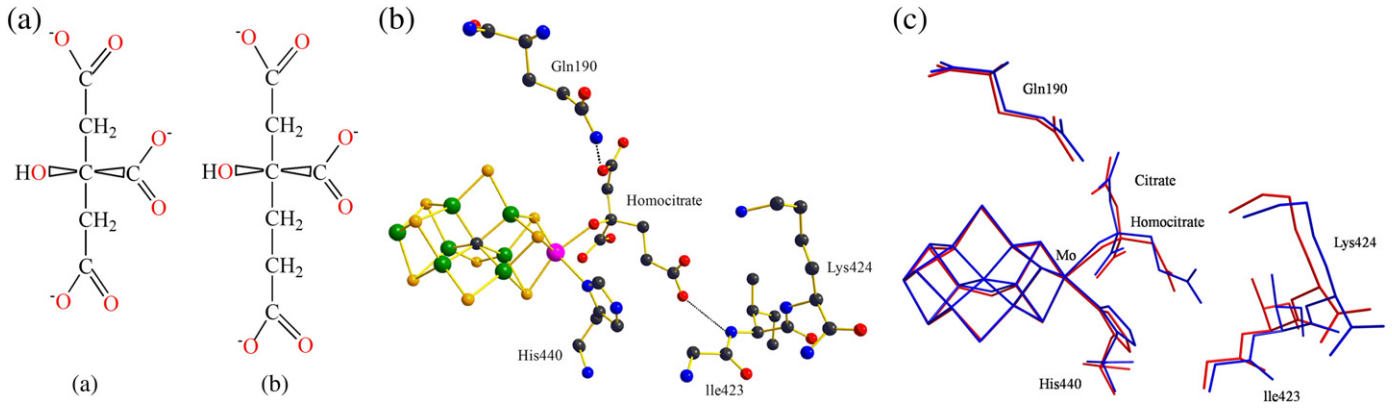

Fig. 1. Left: citrate *vs*. *R*-homocitrate. Middle: ball and stick view of FeMo cofactor and amino acid side chains in vicinity of homocitrate for *Klebsiella pneumoniae* (Kp) nitrogenase. Right: comparison of homocitrate and citrate binding in Kp nitrogenase.

2. Experimental section

2.1. Materials and synthetic methods

Potassium molybdate (99%) and ^{18}O-water were purchased from Sigma. ^{92}Mo- and ^{100}Mo-enriched molybdenum oxides were purchased from Isoflex. Racemic homocitric acid-γ-lactone was prepared *via* a reported synthetic route [19]. The lactone compound was further purified from ethyl acetate and *n*-hexane mixed-solvents.

Homocitrato molybdenum(VI) complexes $K_2[MoO_2(R,S\text{-}H_2\text{-homocit})_2]\cdot 2H_2O$ (**1**), and the ^{92}Mo (**2**) and ^{100}Mo (**3**) isotopomers were synthesized starting from the total synthesis of *R,S*-homocitric acid γ-lactone as shown in Scheme 1. The ^{18}O-γ-carboxy (**4**) isotopomer was prepared starting from the delactonization of *R,S*-homocitric acid γ-lactone in ^{18}O-water.

The *R,S*-homocitric acid γ-lactone (0.21 g, 1.1 mmol) was dissolved in a minimal amount of water. The pH was adjusted to 11 by addition of 5.0 M potassium hydroxide to generate the acyclic homocitrate. The mixture was stirred for two days to complete the hydrolysis at room temperature. Potassium molybdate (0.12 g, 0.50 mmol) was then added and the solution was stirred for another 4 h. The pH value of the solution was adjusted to 2.5 to induce complex formation. Since complex **1** is very soluble in water, potassium chloride could be precipitated first and removed by filtration. Complex **1** was crystallized after evaporation of solvent at room temperature. Yield: 0.15 g (46%). Elemental analyses were acquired using EA 1110 elemental analyzers. Calculated for $C_{28}H_{40}O_{36}K_4Mo_2$: C, 22.4%; H, 3.1%, found: C, 22.0%; H, 3.2%.

In a similar procedure, ^{92}Mo- and ^{100}Mo-enriched oxides (0.25 mmol) were dissolved in 5.0 M potassium hydroxide respectively. The resulting isotopically labeled molybdates were reacted with hydrolyzed homocitrate, and then the pH value of the solutions was titrated to 2.5. Complexes **2**, **3** and **4** were obtained with yields of 40%, 45%, and 41% respectively.

The preparation of molybdenum homocitrates depends mainly on having the required proportions of molybdate and ligand and the correct pH value of the reaction. The suitable pH value is 2–3. A slight excess and complete hydrolysis of the ligand drive the reaction completely and avoid the formation of undesired homocitrate-γ-lactone complexes.

2.2. X-ray data collections, structure solution and refinements

A crystal of (**1**) with dimensions 0.1×0.2×0.2 mm suitable for x-ray structural analysis was obtained as a colorless prism by cooling a saturated solution of (**1**) in a refrigerator (4 °C). X-ray diffraction data were collected on an Bruker Apex II diffractometer with graphite monochromated Mo-Kα radiation at 90 K. A Lorentz-polarization factor, anisotropic decay and empirical absorption corrections were applied. The structure was solved and refined by full-matrix least-squares procedures [20] with anisotropic thermal parameters for all the non-hydrogen atoms. H atoms were located from difference Fourier map and refined with use of a riding model. Crystallographic data (without structure factors) for the structure reported in this paper have been deposited with the Cambridge Crystallographic Data Centre (CCDC) as supplementary publication no. CCDC 871473.

2.3. Spectroscopy

The IR spectra were recorded at a resolution of 2 cm^{-1} with a Vertex 70v Bruker FT-IR spectrometer on KBr plates at room temperature. A KBr beam-splitter and a LN_2 cooled broadband MCT (mercury cadmium telluride) detector were used, allowing measurement over the range of 400–4000 cm^{-1}. The sample chamber was evacuated to 0.5 Torr to minimize the absorption of water vapor.

Solution and solid state NMR spectra were acquired at the UC Davis NMR facility using a Bruker AVANCE500 widebore spectrometer equipped with an 11.7 T magnet field. DSS (sodium 2,2-dimethyl-2-silapentane-5-sulfonate) was used as internal reference in solution

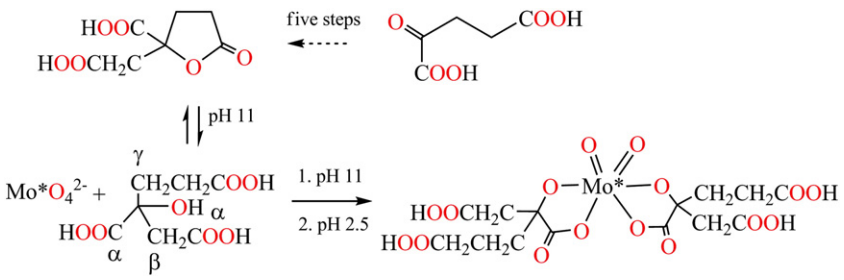

Scheme 1. Synthesis of Mo homocitrate (**1**) and isotopomers: Mo* = Mo, ^{92}Mo (**2**), or ^{100}Mo (**3**).

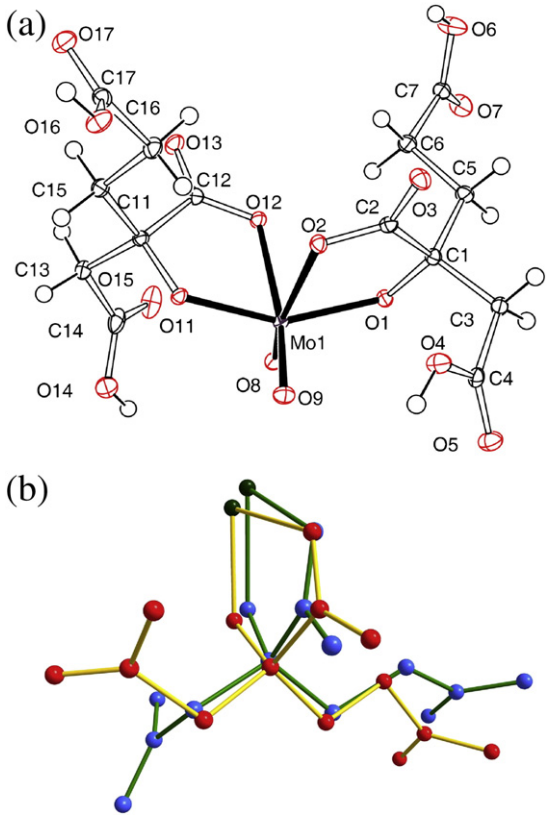

Fig. 2. Left: perspective view of the anion structure of $K_2[MoO_2(R,S\text{-}H_2homocit)_2]\cdot 2H_2O$ (**1**) in Λ_R configuration, thermal ellipsoids are drawn by ORTEP and represent 50% probability surfaces. Right: overlay views of the homocitrate coordination in (**1**) (C in red) and the nitrogenase FeMo-cofactor (C in blue) solved at 1.0 Å resolution [9].

^{1}H NMR and ^{13}C NMR experiments. Solution NMR spectra were taken for measurement after 12 h to obtain a steady spectrum. The concentration of the complex **1** in solution was 0.2 M.

3. Results and discussion

3.1. Description of the molecular structure of (1)

The solid state structure of compound **(1)** comprises discrete potassium cations, *bis*-homocitrate *cis*-dioxomolybdenum anions and water molecules, as shown in Fig. 2. Each Mo is hexacoordinate and exists in *quasi*-octahedral geometry. Selected bond distances and angles for (**1**) are shown in Table 1, while the complete crystallographic data are summarized in the supplemental materials (Table S1).

The homocitrate anions chelate to the Mo *via* α-alkoxy and monodentate α-carboxy groups, while the remaining β- and γ-carboxylic acid groups remain uncomplexed. The homocitrate Mo coordination in (**1**) thus is similar to the homocitrate coordination in the FeMo-cofactor of nitrogenase, as shown in the overlay of the five-member chelated rings in Fig. 2. We note that considerable effort has been expended on the synthesis of chemical models for the FeMo cofactor that emphasize the Mo–S and Fe–S linkages, but relatively less work has been done relevant to the coordination of the tricarboxylic acid [21].

As shown in Table 1, the Mo–O distances in (**1**) vary systematically in the expected fashion. The terminal Mo═O bond lengths are 1.706(1) and 1.714(1) Å, as expected for double bonds. The 104° O═Mo═O angles, are considerably larger than the 90° nominal value for *cis* groups. This is expected from the greater O···O repulsions between oxygen atoms with short bonds to the metal atom. The Mo–O_{alkoxy} distances are longer [1.961(1), 2.007(1) Å], but still consistent with deprotonation of the hydroxy group in the homocitrate anion. Those to α-carboxy oxygen atoms are the longest [2.206(1), 2.211(1) Å], which is a result of the strong *trans* effect of the terminal oxo groups.

As illustrated in Table 2, the Mo–O_{alkoxy} distances in (**1**) are ~0.2 Å shorter than those reported in high resolution nitrogenase structures [8,9]. A longer Mo–O_{alkoxy} bond in the FeMo cofactor seems chemically reasonable, since the oxidation state for Mo is presumed to be Mo(IV) [22], while in (**1**) the Mo is Mo(VI). In contrast, the Mo–$O_{carboxy}$ bond lengths for (**1**) and for the 1.0 Å *Av1* structure are both 2.21 Å. In this case the *trans* effect from the oxo groups in the Mo(VI) complex apparently produces the same bond lengthening as the lower Mo(IV) oxidation state in nitrogenase.

Referring back to Table 1, it is interesting to note that the β-carboxylic acid group forms a very strong intermolecular hydrogen bond with water molecule [O(14)···O(2w), 2.583(2) Å]. Moreover,

Table 2
Comparison of Mo–O distances in (**1**) with those for FeMo cofactor in nitrogenase.

Complex	PDB	M–O_{alkoxy} (Å)	M–$O_{carboxy}$ (Å)	Ref.
(**1**)		1.961(1) 2.007(1)	2.206(1) 2.211(1)	This work
Azotobacter vinelandii N_2ase (1.0 Å) (homocitrate)	3U7Q	2.18	2.21	[9]
Klebsiella pneumoniae N_2ase (1.6 Å) (homocitrate)	1QGU	2.35(2)	2.29(1)	[8]
Klebsiella pneumoniae N_2ase (1.9 Å) (citrate)	1H1L	2.25	2.31	[10]

Table 1
Selected bond distances (Å) and angles (°) for $K_2[MoO_2(R,S\text{-}H_2homocit)_2]\cdot 2H_2O$ (**1**).

Mo–O coordination:					
Mo(1)–O(1)	2.007(1)	Mo(1)–O(2)	2.206(1)	Mo(1)–O(8)	1.714(1)
Mo(1)–O(9)	1.706(1)	Mo(1)–O(11)	1.961(1)	Mo(1)–O(12)	2.211(1)
O(1)–Mo(1)–O(2)	73.75(4)	O(1)–Mo(1)–O(8)	89.56(5)	O(1)–Mo(1)–O(9)	105.07(5)
O(1)–Mo(1)–O(11)	153.50(4)	O(1)–Mo(1)–O(12)	84.76(4)	O(2)–Mo(1)–O(8)	160.56(5)
O(2)–Mo(1)–O(9)	89.93(5)	O(2)–Mo(1)–O(11)	86.48(4)	O(2)–Mo(1)–O(12)	80.97(4)
O(8)–Mo(1)–O(9)	104.26(5)	O(8)–Mo(1)–O(11)	105.85(5)	O(8)–Mo(1)–O(12)	87.79(5)
O(9)–Mo(1)–O(11)	92.10(5)	O(9)–Mo(1)–O(12)	164.28(5)	O(11)–Mo(1)–O(12)	74.66(4)
Hydrogen bonding and cation coordination of β- and γ-carboxy or carboxylic acid groups:					
O(4)···O(13a)	2.520(2)	O(4)–H(4)···O(13a)	164(3)	O(6)···O(3b)	2.588(2)
O(6)–H(6)···O(3b)	168(3)	O(14) ···O(2w)	2.585(2)	O(14)–H(14)···O(2w)	165(3)
O(16)···O(1c)	2.623(2)	O(16)–H(16)···O(1c)	168(3)	O(1w)···O(3d)	2.832(2)
O(1w)–H(1w2)···O(3d)	170(3)	O(2w)···O(13e)	2.719(2)	O(2w)–H(2w1)···O(13e)	158(3)
O(2w)···O(2f)	2.918(2)	O(2w)–H(2w2)···O(2f)	168(3)	K(1)···O(5 g)	2.882(1)
K(1)···O(15 h)	2.641(2)	K(1)···O(17i)	2.743(1)	K(2)···O(5 g)	2.838(1)
K(2)···O(6j)	2.641(2)	K(2)···O(7 h)	2.755(1)	K(2) ···O(14)	2.893(1)
K(2)···O(17i)	2.772(1)				

other β- and γ-carboxylic acid groups form strong intermolecular hydrogen bonds with α-carboxy groups from neighboring homocitrates [O(4)···O(13a), 2.520(2) Å; O(6)···O(3b), 2.588(2) Å], resulting in the formation of a two dimensional coordination polymer. The detailed interactions among β- and γ-carboxylic acid groups with α-alkoxy, α-carboxy groups, and water molecules are shown in Fig. 3. In previous DFT (density functional theory) calculations on an FeMo-cofactor model [23], the γ-carboxy group of *R*-homocitrate is proposed to undergo intramolecular hydrogen bonding with the imidazole ligand on Mo, while the β-carboxy group of the homocitrate ligand is free. This is in contrast with the previous structural reports of the tetranuclear molybdenum homocitrates $(NH_4)_2\,K_2[Mo_4O_{11}(R,S\text{-Hhomocit})_2]\cdot 6H_2O$ and $K_5[Mo_4O_{11}(R,S\text{-Hhomocit})_2]Cl\cdot 5H_2O$ [24], where the β-carboxy group is coordinated. Clearly, the conformational and coordination flexibility of the homocitrate ligand deserves further study.

The β- and γ-carboxylic acid groups in (**1**) are protonated, which is clearly visible in difference maps in the crystallographic data. This is further supported by the charge balance in the complex, and the observed differences in C–O distances (~0.1 Å) between protonated and deprotonated carboxylate oxygens [O(4)–C(4), 1.316(2) Å, O(5)–C(4), 1.218(2) Å; O(6)–C(7), 1.321(2) Å, O(7)–C(7), 1.220(2) Å]. IR bands at 1731 and 1714 cm^{-1} (Fig. 4) also confirm the presence of such protonated β- and γ-carboxy groups in complex **1** as will be discussed below.

3.2. IR spectra and isotopic shifts

IR spectra for (**1**) and various isotopomers are shown in Fig. 4. The 1400–1750 cm^{-1} region is of course a valuable diagnostic for the protonation state of carboxylic acids [25]. Thus, the bands at 1731 and 1713 cm^{-1} correspond to C═O stretches of the protonated β- and γ-carboxylic acid groups of (**1**). The very strong bands of 1701, 1675, 1589 are also associated with carboxylate asymmetric stretches, while the lower frequency features at 1445, 1411, and 1390 cm^{-1} are presumably carboxylate symmetric stretches.

In the region around 900 cm^{-1}, (**1**) shows strong bands of 925.6 and 894.8 cm^{-1} that result from the *cis*-dioxo Mo cores. The low frequency of symmetric MoO_2 stretching can be explained by the coordination of the oxo groups to the potassium cation. Compared to natural abundance **1**, complex **2** shows red shifts of 2.9 and 2.0 cm^{-1} for $\Delta\nu_{Mo=O}$, while complex **3** shows blue shifts of 2.9 and 1.9 cm^{-1} (Fig. 4b). At lower frequencies, bands around 553 and 540 cm^{-1} are assigned to ν_{Mo-O} vibrations. In this case the isotope shifts were on the order of 1.0 cm^{-1} or less and are not considered reliable.

3.3. Solid and solution NMR studies

The ^1H NMR spectrum shows partially overlapping patterns for the three magnetically and/or chemically non-equivalent CH_2 protons of homocitrate ligands. In theory, two protons in these CH_2 groups are inherently magnetically non-equivalent owing to the adjacent α-carbon atom; this is demonstrated by the ^1H NMR spectrum of (**1**) (Figs. S2) showing two AB quartets around 2.57 ppm. The formation constant for (**1**) was determined from this ^1H NMR spectrum. Specifically, the methylene peaks between 3.1 and 1.8 ppm were integrated. Based on the relative intensities of bound and free homocitrate features, the estimated value of the cumulative formation constant was given by log $K_2 = 5.37$, which shows equlirium between coordinated species **1** and free homocitrate.

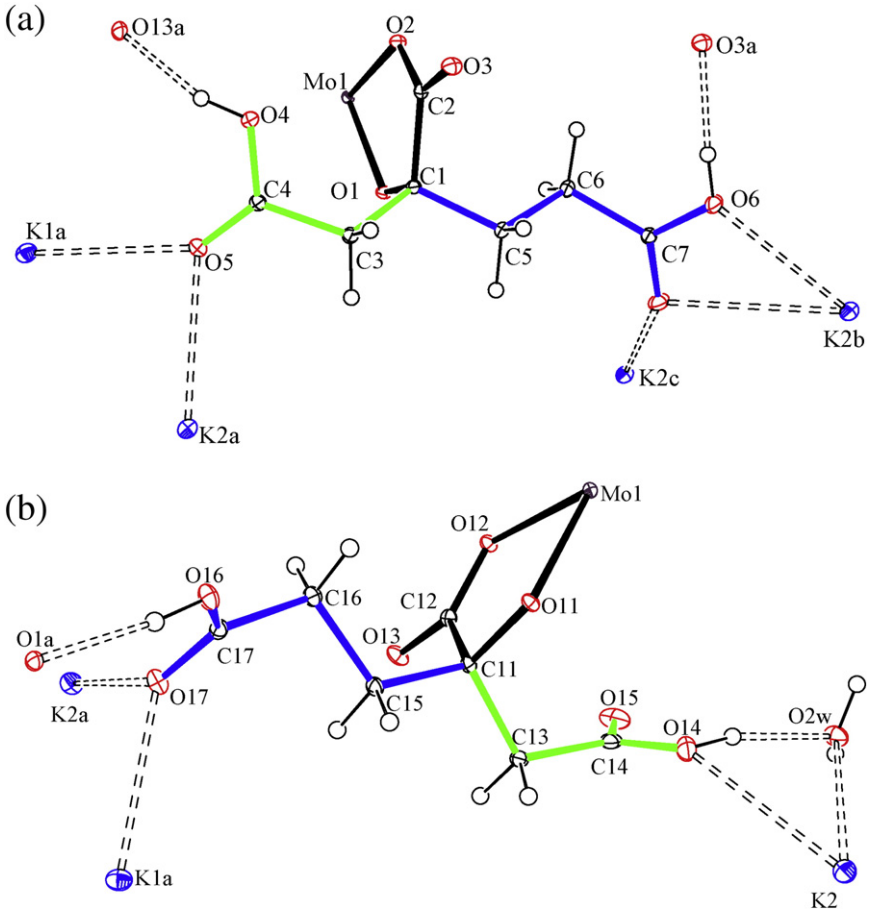

Fig. 3. Environments of β- and γ-carboxylic acid groups in homocitrate portions of (**1**).

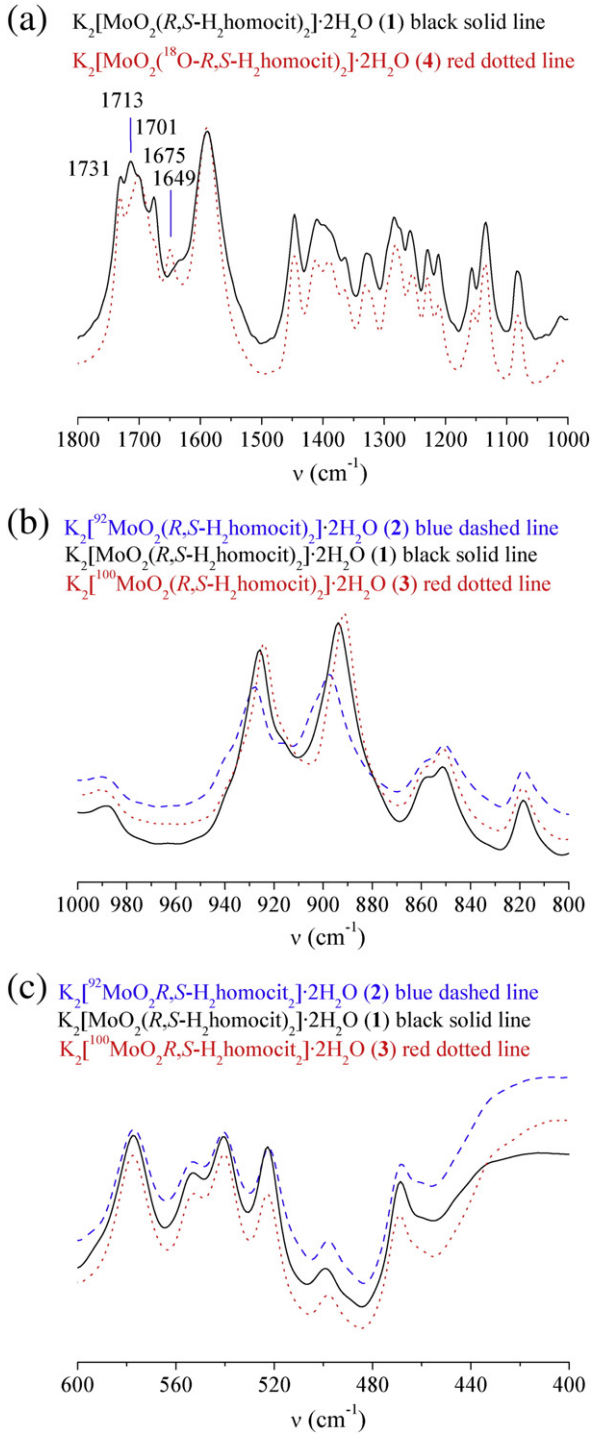

Fig. 4. FTIR spectra of (**1**) and isotopomers. (a) Region between 1000 and 1800 cm^{-1}, comparing (**1**) (black solid line) with isotopomer with ^{18}O γ-carboxylate [4] (red dotted line), (b) region between 800 and 1000 cm^{-1}, comparing (**1**) (black solid line), (**2**) (blue dashed line), and (**3**) (red dotted line), (c) region between 400 and 600 cm^{-1}, comparing (**1**) (black solid line), (**2**) (blue dashed line), and (**3**) (red dotted line).

Due to the overlap of features in the ^1H spectrum, a further study of ^{13}C NMR was carried out. The observed peak positions for (**1**) in the solid state and in solution by ^{13}C NMR spectra are listed in Table 3, and the NMR data for the free homocitric acid-γ-lactone and the potassium homocitrate are also included in the same table for comparisons.

Fig. 5 shows the solid and solution ^{13}C NMR spectra of (**1**) and the NMR of homocitric acid γ-lactone in solid and potassium homocitrate in solution. Different peaks in the spectra correspond to different types of carbons. Taking homocitric acid-γ-lactone (Fig. 5, top) as an example, the peak at 82.8 ppm corresponds to the carbon in the alkoxy group; while the highest 177.9 ppm peak derives from the α-carboxy group. Those at 177.2 and 176.2 ppm are for β- and γ-carboxy ($-CO_2$) groups respectively. The lowest values at 41.4, 29.7 and 27.2 ppm are the peaks for methylene ($-CH_2-$) groups. These solid-state and solution ^{13}C NMR spectra provide valuable information on the coordination environment and the conversions of **1** in solution.

By comparison with the ^{13}C NMR spectrum of the free homocitric acid-γ-lactone, (**1**) gives only one set of ^{13}C NMR signals in the solid state without decomposition, which can be attributed to the coordinated homocitrate in monomeric form. The spectrum shows an obvious downfield shift with respect to the corresponding carbons of free homocitric acid γ-lactone in the solid (Fig. 5, top). As summarized in Table 3, the coordinated α-alkoxy (Δδ 6.3, 4.2 ppm) and α-carboxy (Δδ 7.5, 4.2 ppm) carbons show much larger shifts compared with the corresponding groups in the γ-lactone than do the uncoordinated β- and γ-carboxy carbons (Δδ = 2.0 and −2.5 ppm).

The solution ^{13}C NMR spectrum of (**1**) is similar to that in solid. However, it gives two sets of resonances. Looking at the region around 75–90 ppm, the stronger set corresponds to that of coordinated (**1**) in the solid, which can be attributed to the resonances of the monomeric Mo-homocitrate species in solution. The weaker set at high field, not shown in Table 3, could be derived from decomposition of a bound monomeric species, as that for potassium homocitrate solution. The peak of 77.6 ppm in the high field region is assigned to alkoxy carbon of free ligand. Careful analysis of the solution ^{13}C NMR spectrum in the highfield region shows that there is a small peak at 180.7 ppm, which could be assigned to the free α-carboxy group of homocitrate. The uncoordinated β- and γ-carboxy peaks are mixed with the coordinated species peaks.

The dissociated species could be fully assigned in the spectrum, which can thus serve as an internal reference of free ligand. This is further supported by the comparison between the ^{13}C NMR spectrum for complex **1** and that for potassium homocitrate (Fig. 5, bottom). The dissociated ligand gives obvious downfield shifts for the β- and γ-carboxy groups relative to the free lactone with two acidic groups. This is attributed to the basic medium of potassium homocitrate. Its hydroxy group appears at 79.3 ppm in high field region.

In general, solution ^{13}C NMR downfield shifts in the monomeric Mo homocitrate **1** with respect to dissociated homocitrate are in the decreasing order of α-alkoxy (12.8 ppm) > α-carboxy (6.2 ppm) > β-carboxy (~0 ppm) > γ-carboxy group (~0 ppm) as shown in Table 1. Although α-alkoxy and α-carboxy groups are not strictly comparable, this observation is consistent with the increasing trend in their Mo–O lengths (as measured by X-ray structural analysis) and the decreasing trend in the corresponding bond strengths.

In aqueous solution, the Mo^{6+} complex undergoes acid–base equilibration rapidly and can transform between the complex and free homocitrate ligand, as shown by the ^{13}C NMR measurements in solution. Thus complex **1** also undergoes association-dissociation equilibrium in addition to acid–base equilibrium in solution to give complexed and free homocitrate ligands. The finding here that complex **1** in solution rapidly forms a complex bound with homocitrate ligand as well as free homocitrate may be relevant to homocitrate interactions with molybdenum in nitrogenase. A model for extracted FeMo-co in NMF (N-methylformamide) is thus proposed as shown in Fig. 6, which proposes two kinds of equilibriums between bound homocitrato FeMo-co and the substituted NMF solvent or substrate molecules.

4. Summary

A mononuclear dioxo molybdenum complex with bidentate coordination from two homocitrate anions has been synthesized and isolated from aqueous solution, under controlled conditions of reactant ratio and pH value using the ^{13}C NMR monitoring as a guide. The complex

Table 3
Solid and solution ^{13}C NMR data (in ppm) of (**1**) and various homocitrates.[a]

Compound	≡CO/ ≡COH	$(CO_2)_\alpha$	$(CO_2)_\beta$	$(CO_2)_\gamma$	$(-CH_2-)_\beta$	$(-CH_2-)_\gamma$
Homocitric acid γ-lactone solid	82.8	177.9	177.2	176.2	41.4	29.7, 27.2
(**1**) — solid	89.1(6.3)	185.4(7.5)	179.2(2.0)	173.7(−2.5)	46.4(5.0)	38.3(8.6),37.9(8.2)
	87.0(4.2)	182.1(4.2)			45.8(4.4)	32.0(5.0),29.6(2.4)
Homocitric acid γ-lactone solution	83.5	176.5	172.5	170.5	41.7	31.9, 28.3
Potassium homocitrate solution	79.3	185.8	184.4	182.3	48.8	38.1, 35.0
(**1**) — solution	90.3(12.8)	186.9(6.2)	181.0	177.2	46.2	36.4, 36.3
			180.4	176.6	45.5	32.0, 31.7
$K_2(NH_4)_2[Mo_4O_{11}(Hhomocit)_2]$ $\cdot 6H_2O$ solution [24]	90.0	186.5	181.8	180.7	47.7	37.1, 31.7

[a] Δδ values are given in parentheses.

has been characterized by single crystal x-ray diffraction, FT-IR, and ^{13}C NMR spectroscopy in solution and the solid state, and each technique offered results relevant to homocitrate chemistry in nitrogenase.

The x-ray crystallographic structure revealed that (**1**) possesses the same type of coordination by the 2-alkoxo group and by the monodentate α-carboxylate group as seen in nitrogenase. It also showed the tendency of the remaining β- and γ- carboxylates to engage in H bonding, in this case yielding a two dimensional polymeric structure. The infrared spectrum showed the strength of this technique for addressing the protonation and or ligation status of the carboxylate side chains. Of special note is a band seen for (**1**) at 1675 cm^{-1}, which may be related to the bands seen at 1686 and 1677 cm^{-1} in recent photolysis studies of CO-inhibited nitrogenase [26].

The NMR spectrum of (**1**) shows that it undergoes an equilibrium between the free ligand and the coordinated species in solution. This suggests that the coordinated α-alkoxy and α-carboxy groups are relatively labile in solution. This finding indicates that the molybdenum homocitrate coordination to the FeMo cofactor will have a similar or even greater lability, since it presumably involves a Mo(IV) rather than Mo(VI) ion. This lability may be a factor in the nitrogenase mechanism [27]. It is certainly relevant to the biosynthesis and insertion of the FeMo-cofactor into nitrogenase.

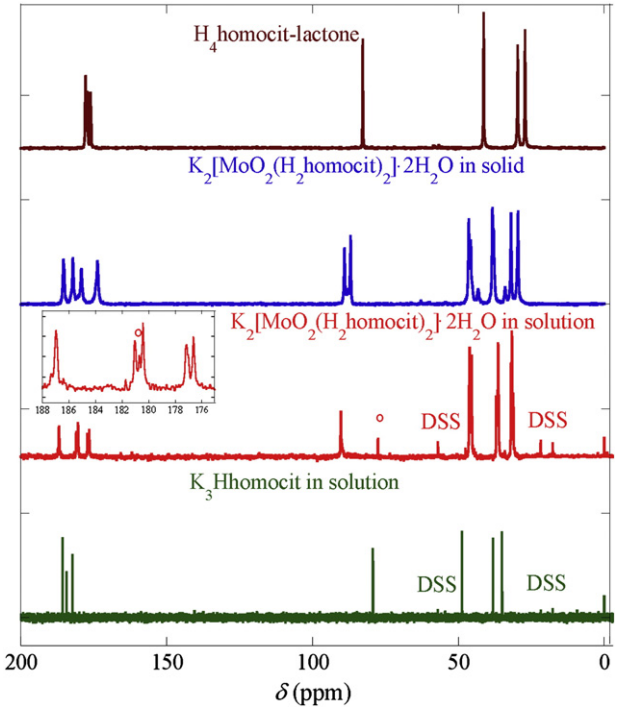

Fig. 5. Solid state and solution ^{13}C NMR spectra of (**1**) compared with potassium homocitrate and homocitric acid γ-lactone.

Abbreviations

H_2homocit	Homocitrate dianion
H_4cit	Citric acid
H_3mal	Malic acid
NMF	N-methylformamide
DFT	Density functional theory

Acknowledgments

This work was supported by (US) National Institute of General Medical Sciences (GM-65440 to SPC), US DOE Office of Biological and Environmental Research (SPC) and the National Science Foundation of China (21073150 to ZHZ). The LBNL work is under DOE contract DE-AC02-05CH11231.

Appendix A. Supplementary data

Supplementary data to this article can be found online at http://dx.doi.org/10.1016/j.jinorgbio.2012.10.001.

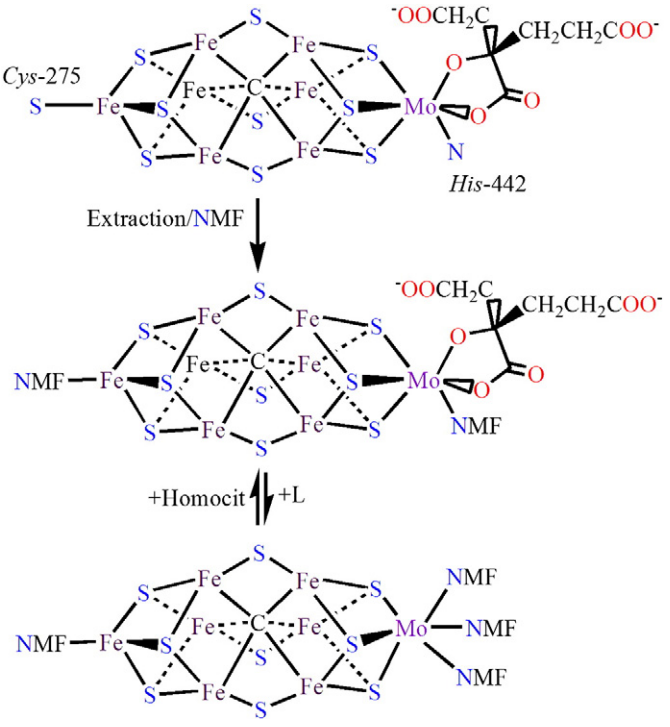

Fig. 6. Proposed lability of homocitrate chelate for extracted FeMo-co in NMF.

References

[1] V.K. Shah, W.J. Brill, Proc. Natl. Acad. Sci. U. S. A. 74 (1977) 3249–3253.
[2] Y.L. Hu, M.W. Ribbe, Coord, Chem. Rev. 255 (2011) 1218–1224.
[3] L.M. Rubio, P.W. Ludden, Annu. Rev. Microbiol. 62 (2008) 93–111.
[4] Y.L. Hu, M.W. Ribbe, Microbiol. Mol. Biol. Rev. 75 (2011) 664.
[5] E.M. Shepard, E.S. Boyd, J.B. Broderick, J.W. Peters, Curr. Opin. Chem. Biol. 15 (2011) 319–327.
[6] P.C. Dos Santos, D.R. Dean, Y.L. Hu, M.W. Ribbe, Chem. Rev. 104 (2004) 1159–1173.
[7] J.K. Kim, D.C. Rees, Nature 360 (1992) 553–560.
[8] S.M. Mayer, D.M. Lawson, C.A. Gormal, S.M. Roe, B.E. Smith, J. Mol. Biol. 292 (1999) 871–891.
[9] T. Spatzal, M. Aksoyoglu, L. Zhang, S.L.A. Andrade, E. Schleicher, S. Weber, D.C. Rees, O. Einsle, Science 334 (2011) 940.
[10] S.M. Mayer, C.A. Gormal, B.E. Smith, D.M. Lawson, J. Biol. Chem. 277 (2002) 35263–35266.
[11] P.A. McLean, R.A. Dixon, Nature 292 (1981) 655–656.
[12] P.A. McLean, B.E. Smith, R.A. Dixon, Biochem. J. 211 (1983) 589–597.
[13] J. Imperial, T.R. Hoover, M.S. Madden, P.W. Ludden, V.K. Shah, Biochemistry 28 (1989) 7796–7799.
[14] P.D. Christie, H.I. Lee, L.M. Cameron, B.J. Hales, W.H. Orme-Johnson, B.M. Hoffman, J. Am. Chem. Soc. 118 (1996) 8707–8709.
[15] P.M.C. Benton, S.M. Mayer, J. Shao, B.M. Hoffman, D.R. Dean, L.C. Seefeldt, Biochemistry 40 (2001) 13816–13825.
[16] P.M.C. Benton, L. Laryukhin, S.M. Mayer, B.M. Hoffman, D.R. Dean, L.C. Seefeldt, Biochemistry 42 (2003) 9102–9109.
[17] Z.Y. Yang, L.C. Seefeldt, D.R. Dean, S.P. Cramer, S.J. George, Angew. Chem. 123 (2011) 286–289.
[18] R. Sarma, B.M. Barney, S. Keable, D.R. Dean, L.C. Seefeldt, J.W. Peters, J. Inorg. Biochem. 104 (2010) 385–389.
[19] H.B. Chen, L.Y. Chen, P.Q. Huang, H.K. Zhang, Z.H. Zhou, K.R. Tsai, Tetrahedron 63 (2007) 2148–2152.
[20] G.M. Sheldrick, Acta Crystallogr. A 64 (2008) 112–122.
[21] P.V. Rao, R.H. Holm, Chem. Rev. 104 (2004) 527–559.
[22] P.E. Doan, J. Telser, B.M. Barney, R.Y. Igarashi, D.R. Dean, L.C. Seefeldt, B.M. Hoffman, J. Am. Chem. Soc. 133 (2011) 17329–17340.
[23] K.L.C. Grönberg, C.A. Gormal, M.C. Durrant, B.E. Smith, R.A. Henderson, J. Am. Chem. Soc. 120 (1998) 10613–10621.
[24] Z.H. Zhou, S.Y. Hou, Z.X. Cao, K.R. Tsai, Y.L. Chow, Inorg. Chem. 45 (2006) 8447–8451.
[25] J.J. Max, C. Chapados, J. Phys. Chem. A 108 (2004) 3324–3337.
[26] L. Yan, C.H. Dapper, S.J. George, H.X. Wang, D. Mitra, W.B. Dong, W.E. Newton, S.P. Cramer, Eur. J. Inorg. Chem. (2011) 2064–2074.
[27] M.C. Durrant, A. Francis, D.J. Lowe, W.E. Newton, K. Fisher, Biochem. J. 397 (2006) 261–270.